Influence of higher-order deformations in the ^{34}S + ^{168}Er fusion reaction

C. R. Morton, A. C. Berriman, R. D. Butt, M. Dasgupta, D. J. Hinde, A. Godley, and J. O. Newton

*Department of Nuclear Physics, Research School of Physical Sciences and Engineering, Australian National University,
Canberra ACT 0200, Australia*

K. Hagino

Yukawa Institute for Theoretical Physics, Kyoto University, Kyoto 606-8502, Japan

The shape of the measured barrier distribution for the ^{34}S + ^{168}Er reaction is analyzed using the coupled-channels description. The ^{168}Er nucleus is a good candidate to test current fusion models description of deformation since it has a large quadrupole deformation with an insignificant hexadecapole deformation. Coupling to weaker channels, the 2_1^+ state in ^{34}S, the 3_1^- state in ^{168}Er, and the pair neutron transfer channel, all were found to have little influence on the barrier distribution. A successful description of the barrier distribution was only obtained after the hexacontatetrapole deformation term in ^{168}Er (β_6^T) was included in the coupling scheme. However, a positive value for β_6^T was needed where the macroscopic-microscopic model predicts a negative one.

I. INTRODUCTION

The influence of the internal structure of nuclei on the probability for heavy-ion fusion is well established. Coupling of the relative motion of projectile and target nuclei to internal nuclear degrees of freedom produces a distribution of fusion barriers that replaces the single fusion barrier which results when these couplings are not included [1–4]. The degrees of freedom that affect fusion include the deformation of one or both reactants, the excitation of collective surface vibrational modes, and single or multiple-nucleon transfer channels.

In general, collective modes involving large numbers of nucleons play the major role in determining the shape of the fusion barrier distribution. Evidence for this can be seen in the measured barrier distribution for the system ^{16}O + ^{144}Sm [5,6], for example, where the lowest energy octupole state in ^{144}Sm accounted for a large part of the structure in the experimental barrier distribution, whilst the transfer channels had only a relatively minor effect at energies in the barrier region. This difference is due to the weakness of the coupling of one- or two-particle transfer channels relative to the coupling strength of the collective modes [7]. This does not imply, however, that there are no significant effects of transfer on fusion. The effects of positive (effective) Q-value transfers, when present, are most evident in the enhancement of the fusion cross section at energies well below the average fusion barrier B_0, since they determine the energy of the lowest barrier [3,6,8].

Two examples of the sensitivity of the fusion barrier distribution to the effects of deformation are the ^{16}O + ^{154}Sm [6,9] and ^{16}O + ^{186}W reactions [6,10]. Calculations which could reproduce the measured barrier distributions required not only a quadrupole deformation term but also inclusion of a hexadecapole term, where the sign of the latter was responsible for the difference in shapes of the two barrier distributions [compare the solid lines in Figs. 1(a) and 1(b)]. Although the quadrupole and hexadecapole degrees of freedom are responsible for a large part of the barrier distribution's

shape, there are small differences between the shape of the theoretical and experimental barrier distributions at center-of-mass energies $E_{\text{c.m.}} \lesssim B_0$. It was shown in Ref. [6] however, that if additional coupling to vibrational states and transfer channels were included in the theoretical model, then a better reproduction of the shape of the measured barrier distributions resulted. The calculations of Ref. [6] are shown by the dashed lines in Figs. 1(a) and 1(b) for the ^{154}Sm and ^{186}W targets, respectively. The deformation parameters obtained from these fits to the data were found to be in closer agreement with published (nonfusion) values [11] than those calculations which excluded the additional couplings.

However, as recognized in Refs. [6,10], the addition of *any* weak couplings may result in an improvement in the reproduction of the shape of the measured barrier distribu-
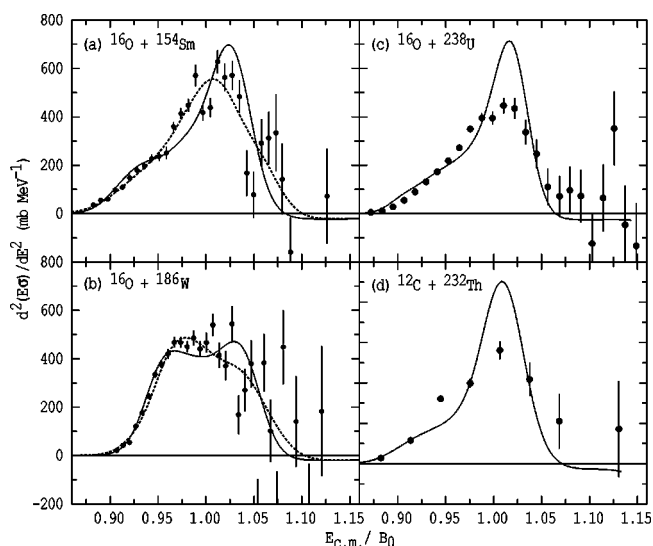

FIG. 1. Fusion barrier distributions for a range of deformed nuclei in the reactions (a) ^{16}O + ^{154}Sm [6,9], (b) ^{16}O + ^{186}W [6,10], (c) ^{16}O + ^{238}U [12], and (d) ^{12}C + ^{232}Th [13].

tion. The resulting deformation parameters from the fit to the fusion data are in better agreement with nonfusion values since, to a large extent, the additional couplings in ^{154}Sm and ^{186}W mimic the changes in the deformation parameters required to reproduce the barrier distribution shape.

In other measurements involving deformed target nuclei, a discrepancy between the theoretical and experimental barrier distributions in the region $0.94 \lesssim E_{c.m.}/B_0 \lesssim 1.0$ MeV was found in possibly four different systems. Examples are shown in Figs. 1(c) and 1(d) for the ^{16}O$+$ ^{238}U [12] and ^{12}C$+$ ^{232}Th [13] reactions, respectively. Is this discrepancy due to coupling to weaker channels or to some deficiency in the theoretical description of fusion involving deformed nuclei? Or are the measured fusion barrier distributions sensitive to higher-order deformations, such as the β_6^T deformation, presently absent from the analyses of fusion involving deformed nuclei? A recent paper [14] addressed this last question by examining the influence of the β_6^T deformation on fusion for the ^{16}O$+$ ^{154}Sm, ^{186}W, and ^{238}U systems. However, the disadvantage of this analysis [14] was that all the nuclei involved in the study have large β_4^T deformations, which meant it was difficult to isolate the effects due to the β_6^T term from the β_4^T contributions.

In order to investigate the influence of higher-order deformations, such as the β_6^T term, a target nucleus with a pure prolate deformation should be chosen, to avoid distortion due to a hexadecapole component. The ^{168}Er nucleus is a good candidate since it has a large prolate deformation and a hexadecapole deformation that is expected to be zero, or very small [15,16]. The β_3^T vibrational mode in ^{168}Er is also weakly coupled compared to the ^{238}U target nucleus where this mode is significant. Additionally, it is desirable to choose a reaction that involves a projectile nucleus with a high charge because the width of the barrier distribution is proportional to $Z_1 Z_2$, which produces a "magnification" of the coupling effects.

The reaction ^{34}S$+$ ^{168}Er is suitable based on the above criteria. It was recently used [17,18] in a measurement of the fusion cross sections, and the fusion barrier distribution, for input into transition state model calculations used to test fission models at large angular momenta. In this paper, the fusion barrier distribution for ^{34}S$+$ ^{168}Er from Refs. [17,18] is analyzed to examine the role higher-order deformations play in heavy-ion fusion. Details of the experiment and results for the ^{34}S$+$ ^{168}Er measurement have been published [18]. In Sec. II that follows, the sensitivity of the ^{34}S $+$ ^{168}Er barrier distribution to the nuclear potential parameters is examined. Then the effects of deformation on the barrier distribution are calculated in Sec. III after checking the adequacy of the approximate treatment of the excitation energies of states in ^{168}Er. In Sec. IV, the effects of coupling to the octupole vibration in ^{168}Er, and states in ^{34}S is examined, followed by a discussion on the effects of transfer couplings, and the conclusion in Sec. V.

II. NUCLEAR POTENTIAL PARAMETERS

One uncertainty concerning the theoretical description of heavy-ion fusion is the true form of the nuclear potential
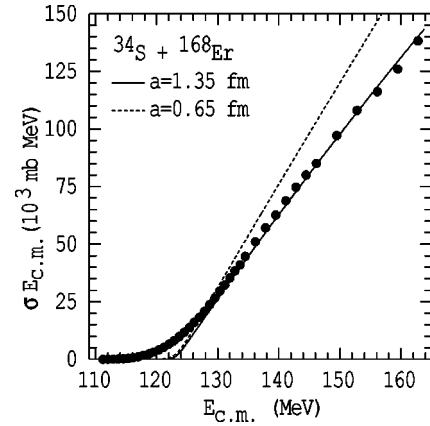

FIG. 2. Linear plot of $\sigma E_{c.m.}$ for the measured fusion cross-sections (solid points) for ^{34}S$+$ ^{168}Er compared with two single-barrier penetration model calculations, one with $a=1.35$ fm (solid line), and the other with $a=0.65$ fm (dashed line).

between interacting nuclei in the absence of channel coupling. In fusion analyses, an energy-independent nuclear potential of Woods-Saxon form has often been used, with

$$V(r) = -\frac{V_0}{1 + \exp[(r - r_0 A_P^{1/3} - r_0 A_T^{1/3})/a]}, \quad (1)$$

where V_0 is the depth, r_0 is the radius parameter, and a is the diffuseness of the nuclear potential. One method for determining the parameters of the Woods-Saxon potential is the procedure described in Ref. [6], where the fusion cross sections σ have been fitted with a single barrier penetration model at energies $\approx 10\%$ above the average barrier where there is no longer any significant barrier strength. The rationale behind this procedure is that at energies well above the average barrier the calculated cross sections are very sensitive to B_0 but relatively insensitive to the channel couplings, thus enabling an estimate of the "bare" nuclear potential.

With the advent of precise fusion data, even this small sensitivity to the channel couplings at higher energies was measurable, and was dealt with usually in one of two ways. In calculations that included couplings with excitation energies smaller than the curvature of a single barrier $\hbar\omega_0$, a small increase in the fusion barrier was made in order to retain the quality of the fit to the high-energy data obtained without the couplings. Where the excitation energies of states was greater than $\hbar\omega_0$, they were not included explicitly in the calculations, since these states only contribute to a renormalization of the "bare" nuclear potential and have no effect on the shape of the barrier distribution [19].

If these higher lying states are included in the calculations, care should be taken not be count their effects twice, or wrong conclusions about the position of average fusion barrier will be drawn. An example of this problem is shown in Ref. [20] where the quoted "average barrier" is several MeV above the *measured* average fusion barrier as determined by their experimental fusion barrier distribution.

The fit to the high-energy fusion cross sections for ^{34}S $+$ ^{168}Er is shown by the solid line in Fig. 2, where the quan-

TABLE I. Parameters for the real nuclear potential for ^{34}S + ^{168}Er [see Eq. (1)].

V_0 (MeV)	r_0 (fm)	a (fm)
392.5	0.80	1.35
292.1	1.10	0.65

tity $\sigma E_{c.m.}$ has been plotted on a linear scale for clarity. The parameters for the nuclear potential obtained from this fit are given in the second row of Table I, noting that the diffuseness obtained was $a = 1.35$ fm. The resulting average barrier is $B_0 = 123.1$ MeV at a barrier radius of $R_B = 11.1$ fm. The diffuseness from this fit is much larger than the results from fits to elastic scattering data in Ref. [11], where the fitted value for the diffuseness was found to be $a = 0.63$ fm. Large values for a, in the range $a = 0.84$–1.35 fm, have also been required to fit data in recent measurements [6,21,22] involving a range of projectile-target combinations. In Ref. [22] an alternative form for the nuclear potential was suggested as a possible explanation for the large values of a. If the nuclear potential fell more rapidly with increasing values of r than the rate suggested by the Woods-Saxon form of Eq. (1), it may be possible to match the potential at large r required to fit the elastic scattering data, while retaining the fit to fusion cross sections at the smaller values of r probed by fusion collisions.

A clue as to the actual value for the diffuseness of the nuclear potential can be obtained from the slope of the fusion excitation function in the tunneling regime. That is, at energies below the lowest barrier, where coupling effects no longer influence fusion. If the diffuseness obtained from fits to elastic scattering is appropriate for fusion, then the fusion excitation function will also have this slope provided the energy is sufficiently below the lowest barrier. If the fusion excitation function falls more rapidly with energy than a calculation with $a = 0.63$ fm, this means fusion takes place through a wider barrier (less penetrability), implying a larger value for a. In the present case, it is difficult to determine the slope of the fusion excitation function because of the large width of the ^{34}S + ^{168}Er barrier distribution, resulting from the target nucleus deformation, and the possible influence of positive Q value transfers. However, other experiments have recently being performed [23], using reactions that have a suitably narrow barrier distribution, and preliminary analysis of this data does support a value for a significantly larger than the elastic scattering results.

A calculation was performed to demonstrate the effect of using a diffuseness smaller than the fusion data require. A value of $a = 0.65$ fm was chosen, which overestimates the measured cross sections at high energies (see the dashed line in Fig. 2). The nuclear potential parameters for this calculation are given in the third row of Table I. The potential parameters were chosen to keep the fusion barrier unchanged at $B_0 = 123.1$ MeV, which meant that R_B was increased from 11.1 to 12.0 fm to compensate. The fusion barrier distribution resulting from a calculation with $a = 0.65$ fm and a quadrupole deformation of $\beta_2^T = 0.338$ [24] only is shown by the dashed line in Fig. 3. The barrier distribution from this
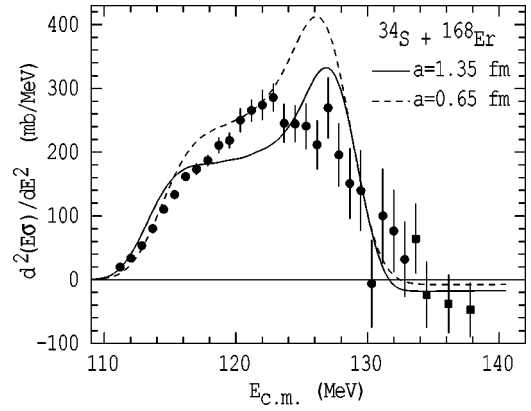

FIG. 3. The measured fusion barrier distribution for ^{34}S + ^{168}Er [18]. Here the second derivative was evaluated with a step length $\Delta E_{c.m.} = 3.33$ MeV (solid circles) or $\Delta E_{c.m.} = 6.66$ MeV (solid squares). Also shown are two CC calculations which are identical except for the nuclear potential parameters, the solid line results from the calculation made with $a = 1.35$ fm, and the dashed line with $a = 0.65$ fm. See text.

calculation also leads to a deterioration in the agreement with measured barrier distribution.

III. EFFECTS OF DEFORMATION ONLY

Having established that a smaller diffuseness parameter made the agreement between the calculated and experimental excitation function and barrier distribution worse, the effects of deformation are examined in this section. Coupled-channels (CC) calculations were performed with the code CCDEGEN [25], which is based on a version of the code CCFULL described in Ref. [26]. In CCDEGEN, the effects of deformation are calculated by coupling to the ground-state rotational band of the deformed target nucleus, using the no-Coriolis approximation [27,28] with the excitation energies of the states in the ground-state band taken to be zero. The no-Coriolis approximation has been shown to be adequate for reactions involving heavy ions [21,29]. These approximations enable the CC equations to be decoupled, and the resulting eigenchannel equations, which correspond to fusion of the (inert) projectile and deformed target nucleus whose symmetry axis is orientated at an angle θ with respect to the beam axis, are solved [14] to obtain the tunneling probability $P_J(E_{c.m.}, \theta)$ for each partial wave $J\hbar$. The fusion cross section is then calculated using

$$\sigma(E_{c.m.}) = \pi \lambdabar^2 \sum_J (2J+1) P_J(E_{c.m.}), \qquad (2)$$

where $P_J(E_{c.m.})$ is the total tunneling probability for each J averaged over all orientations, and is given by

$$P_J(E_{c.m.}) = \frac{1}{2} \int_0^\pi P_J(E_{c.m.}, \theta) \sin \theta \, d\theta. \qquad (3)$$

Equation (3) is exact for the classical situation, where the number of (degenerate) states in the rotor tends to infinity [30]. In actual rotational nuclei, the number of states is finite,

and the integral in Eq. (3) is evaluated up to some maximum value of spin I_{max} (where all spins are even) [30]. This is done using an *n*-point Gaussian integration formula, where $n/2 = (I_{max} + 2)$. For the calculations described in this work, for systems other than ^{34}S + ^{168}Er [see Figs. 1(c) and 1(d)], a total of five states up to the 8^+ state were included, which corresponds to a coupled-channels calculation with five channels. Including states with spins higher than the 8^+ state did not make an appreciable difference to the calculated fusion cross section. For the ^{34}S + ^{168}Er calculations, six states, up to the 10^+ state, were needed to evaluate the integral to the desired accuracy.

To test the zero excitation energy approximation used in these calculations, a comparison was made with a calculation which takes into account the finite excitation energies of the rotational states. The calculation shown by the dashed line in Fig. 4(a) was made with the CC code CCFULL [26], which included coupling to all orders in the deformation parameter for the nuclear coupling potential, with the energy of the first 2^+ in ^{168}Er at 79.8 keV. The excitation energies of higher members of the rotational band were calculated according to the usual formula for a rotating rigid body. The solid line in Fig. 4(a) is the barrier distribution from the CCDEGEN calculation, using the geometric description of Eq. (3). The parameters for the nuclear potential were identical in these two calculations (see the second row of Table I). Both calculations were made with $\beta_2^T = 0.338$ [24] and included coupling to all orders in the deformation parameter for the nuclear coupling potential. The difference between the two calculations is small which can be attributed to the large deformation, or equivalently the low energy of the first excited state in ^{168}Er, although the agreement is not perfect [31]. Having shown numerically that the zero excitation energy approximation in CCDEGEN is a good approximation to better than the accuracy of the data, it was used in all the fusion calculations that follow to test the effects of various deformation parameters.

(1) Quadrupole deformation. The shape of the barrier distribution that results from consideration of the quadrupole deformation only [solid line in Fig. 4(a) with $\beta_2^T = 0.338$] cannot account fully for the shape of the measured barrier distribution. Although the area under the calculation (when $a = 1.35$ fm) matches to within 2–4 % the area under the measured barrier distribution,[1] the latter peaks at a lower energy than the theoretical curve and has a more "triangular" shape. Varying the magnitude of β_2^T does not improve the agreement.

(2) Hexadecapole deformation. Although the hexadecapole deformation for ^{168}Er is expected to be very small, a calculation was performed to ascertain the influence of this degree-of-freedom on the shape of the barrier distribution. The results of two CC calculations are shown by the broken lines in Fig. 4(b), one with $\beta_2^T = 0.338$ and $\beta_4^T = +0.01$ (dashed line) and the other with $\beta_2^T = 0.338$ and $\beta_4^T = -0.01$
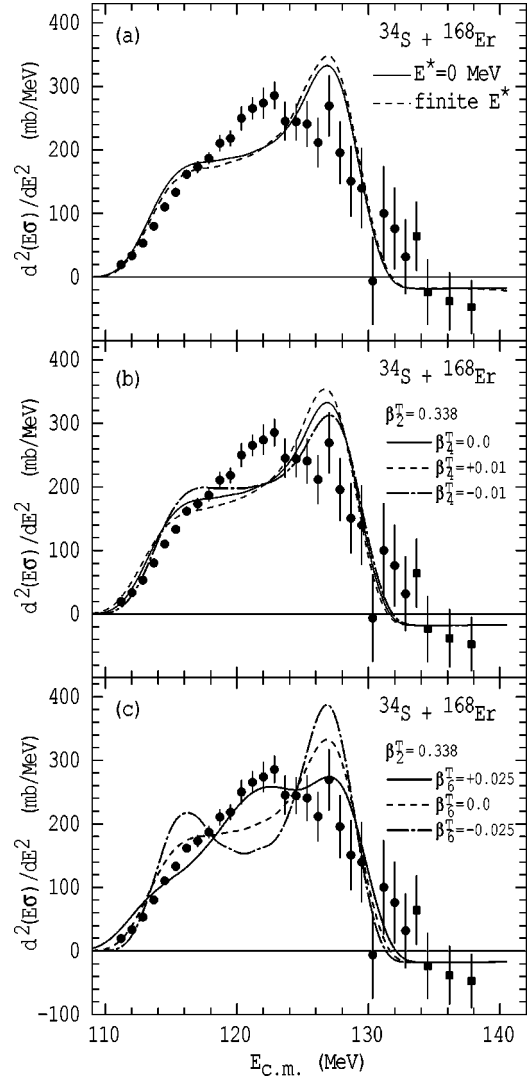

FIG. 4. (a) Test of the zero excitation energy approximation used in the CC code CCDEGEN (solid line) compared with an exact calculation (dashed line). See text for details. (b) Barrier distributions showing the effects of including the β_4^T deformation in addition to β_2^T. The solid line is a CCDEGEN calculation with $\beta_4^T = 0$, the dashed line with $\beta_4^T = +0.01$, and the dot-dashed with $\beta_4^T = -0.01$. (c) Effects of the hexacontatetrapole deformation on the barrier distribution. Shown are CCDEGEN calculations with $\beta_2^T = 0.338$ and $\beta_6^T = 0$ (dashed line), $\beta_2^T = 0.338$ and $\beta_6^T = +0.025$ (solid line), and $\beta_2^T = 0.338$ and $\beta_6^T = -0.025$ (dot-dashed line). Note that β_4^T is zero in each of the calculations shown in panel (c).

(dot-dashed line). These two values for β_4^T span the range of likely values for ^{168}Er, as determined in Ref. [32] where a value of $\beta_4^T = -0.007$ was estimated. Of the resulting range of shapes shown in Fig. 4(b), none lead to a significant improvement in the agreement with the data.

(3) Hexacontatetrapole deformation. Since the effect of the hexadecapole deformation for the ^{168}Er nucleus is small, what then is the effect of the hexacontatetrapole (β_6^T) degree of freedom on fusion? Guidance as to the magnitude and sign of the β_6^T deformation comes from theory. The ground-state shapes for a large number of nuclei have been calcu-

---

[1]The range depends upon the limits taken for evaluation of the integral.

TABLE II. Summary of the β_2^T, β_4^T, and β_6^T deformation parameters for nuclei as indicated.

Nucleus	β_2^T	β_4^T	β_6^T
^{168}Er	+0.338 [24]	−0.007 [32]	−0.025 [32]
^{154}Sm	+0.28 [6]	+0.05 [6]	−0.005 [32]
^{238}U	+0.275	+0.05	−0.015 [32]

lated by Möller, Nix, Myers, and Swiatecki using a global macroscopic-microscopic model [32]. They calculated a value of $\beta_6^T = -0.025$ for ^{168}Er [32], which is a factor 3.5 times larger than the β_4^T estimate for the same nucleus. A CCDEGEN calculation with $\beta_6^T = -0.025$, in addition to the quadrupole deformation ($\beta_2^T = 0.338$), is shown by the dot-dashed line in Fig. 4(c). The β_6^T deformation does have a significant effect on the shape of the barrier distribution, leading to more peaked shapes at each end of the barrier distribution. However, the inclusion of the negative hexacontatetrapole term worsens the agreement with the data.

Another calculation was performed but this time with the opposite sign for the β_6^T deformation. This calculation, with $\beta_2^T = 0.338$ and $\beta_6^T = +0.025$, is represented by the solid line in Fig. 4(c). The inclusion of the β_6^T term with a positive instead of negative sign now improves the agreement with the measured barrier distribution, although all its features are still not completely reproduced.

In the recent work of Ref. [14], Rumin *et al.* investigated the influence of the β_6^T deformation on fusion for the ^{16}O induced reactions on ^{154}Sm, ^{186}W, and ^{238}U. In that work the authors concluded that the *fits* to the measured barrier distributions were improved by inclusion of the β_6^T terms, but in doing so obtained unphysically small β_4^T values for these actinides, contrary to their known hexadecapole deformations. It would be reasonable to conclude that the presence of the β_6^T term compensates for the large reduction in the β_4^T values. A contrasting approach is taken in this work, where the "known" values of β_2^T and β_4^T for ^{168}Er are used rather than allowed to vary as free parameters in a fit to the barrier distribution. The basis for this approach is that the β_2^T value has been determined experimentally [24], and the theoretical basis for β_4^T being close to zero is well established, since Er is midpoint the region of Z where β_4^T changes from a positive value (Sm and Gd, for example) to a negative one (Yb and Hf) [15,16].

An advantage the present study has over the analysis of Rumin *et al.* [14] is that the β_4^T for ^{168}Er nucleus is approximately seven times smaller than the β_4^T for the ^{154}Sm and ^{238}U nuclei (see Table II), implying there is very little influence of the hexadecapole deformation on the shape of the barrier distribution for ^{34}S + ^{168}Er. In addition, the estimated [32] magnitude for the β_6^T value for ^{168}Er is around 1.5 times the estimate for ^{238}U and 5 times the β_6^T for ^{154}Sm, increasing the possibility that fusion barrier distribution might be sensitive to the effects of this deformation parameter. When the deformation parameters for each nucleus are placed into the multipole expansion of the nuclear part of the coupling

interaction, the hexacontatetrapole term for ^{168}Er is 3.6 times larger than its hexadecapole term, compared to ^{238}U case where the hexacontatetrapole term is 3.4 times *smaller* than its hexadecapole term. So if the ^{16}O + ^{238}U barrier distribution is sensitive to the presence of the β_4^T in ^{238}U, then it may not be unexpected that the barrier distribution for ^{34}S + ^{168}Er is sensitive to the β_6^T deformation in ^{168}Er.

Although using the magnitude for β_6^T from Möller's estimate produced a good description of the measured barrier distribution, the sign had to be inverted in order to achieve this agreement. In Ref. [14], a similar problem arose, where the sign for β_6^T was also found to be opposite to theoretical predictions, after *fits* to the experimental barrier distributions for ^{16}O + ^{238}U and ^{16}O + ^{154}Sm were performed. An attempt was made to address this sign problem by refitting the barrier distributions with, in addition to the β_2^T, β_4^T, and β_6^T terms, coupling to the octupole vibration of ^{238}U and ^{154}Sm. This calculation then matched the theoretically predicted sign for β_6^T but, as discussed above, unphysically small values for β_4^T [14] were obtained. In the case of ^{34}S + ^{168}Er, it was not possible to explain its sign problem by coupling to the 3_1^- state in ^{168}Er, because this state couples so weakly (see Sec. IV below).

To check that the positive sign required is not due to truncation of higher-order terms in the Coulomb coupling equation, another calculation was performed which included the $(\beta_2^T)^3$ terms of the Coulomb interaction. It was found that these terms had a very minor effect on the calculated barrier distribution for ^{34}S + ^{168}Er, corresponding to a change by a "linewidth" in the shape of the barrier distribution, and could not explain why a positive sign for β_6^T was needed.

Whether or not the measured barrier distribution for ^{34}S + ^{168}Er can determine the sign of the β_6 deformation in ^{168}Er remains an open question. The macroscopic-microscopic calculations of Möller *et al.* [32] predict strong negative β_6 deformation in the $N \approx 100$, $Z \approx 60$ region, however, it is worth noting the comment in Ref. [32] that the behavior of hexacontatetrapole deformation across the chart of the nuclides is less regular than that of the lower order, even (β_2, β_4) multipole distortions.

Since the size of the deformation parameters extracted from the measured barrier distributions can depend upon the presence or absence of weaker couplings [6], the effects of these channels are investigated in the next section.

IV. COUPLING TO WEAKER CHANNELS

In this section, coupling to channels other than the rotational coupling is considered, starting with the octupole vibration in ^{168}Er. The dashed line in Fig. 5(a) is a CCDEGEN calculation with $\beta_2^T = 0.338$, $\beta_6^T = +0.025$, and with the first 3^- state in ^{168}Er. The energy for this state is 1431 keV and the coupling strength was taken to be $\beta_3^T = 0.064$, obtained from the measured $B(E3) \uparrow$ value [33] with a radius for ^{168}Er taken as $1.06A_T^{1/3}$ fm [6]. The barrier distribution with the octupole coupling is only slightly different to the calculation without it [solid line in Fig. 5(a)] implying that this
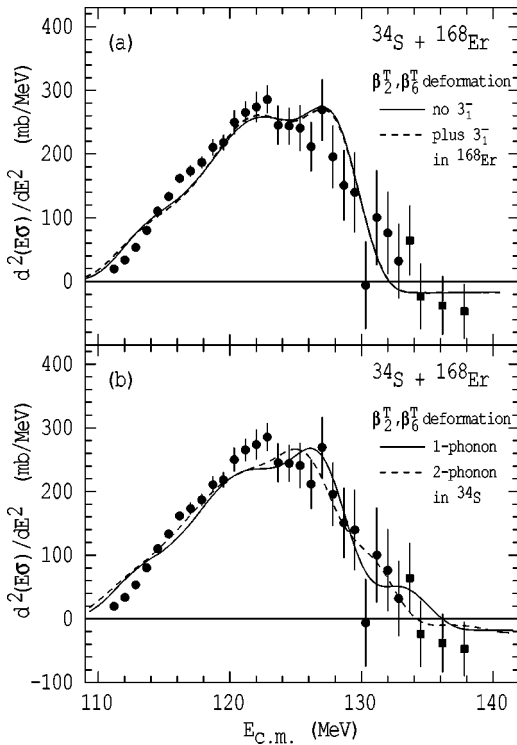
FIG. 5. (a) The effect on the barrier distribution when the 3_1^- state in ^{168}Er is taken into account (dashed line), with $\beta_2^T = 0.338$ and $\beta_6^T = +0.025$. Also shown is the same calculation without the 3_1^- state (solid line). (b) Barrier distributions for two calculations with β_2^T and β_6^T deformation plus coupling to the 2_1^+ state in ^{34}S (solid line) and, in addition, coupling to the two-phonon state in ^{34}S (dashed line).

FIG. 6. Comparison of the barrier distribution that results from coupling to the first 2^+ state in ^{34}S only (dashed line) and target deformation only (solid line).

state does not play a major role in the coupling scheme. This is expected since the coupling strength for the octupole state is very weak. Similarly, coupling to higher lying states, for example, γ and β vibrations, should have very little influence on the barrier distribution, as shown to be the case in Ref. [14] for ^{16}O induced reactions on the deformed ^{154}Sm, ^{186}W, and ^{238}U targets. The effects of coupling to more exotic modes of excitation [34], such double-β vibrations (two-phonon collective excitations), have not been examined.

(4) Coupling to states in ^{34}S. Up to this point in the analysis, ^{34}S has been treated as inert in the calculations. However, low lying states in ^{34}S will contribute to the channel coupling, and the size of their influence should be calculated. The barrier distribution shown by the solid line in Fig. 5(b) is a calculation which includes β_2^T and β_6^T deformation in the target, plus coupling to the 2_1^+ state in ^{34}S, whose energy is 2.127 MeV with a coupling strength of $\beta_2^P = 0.25$. Also shown by the dashed line in Fig. 5(b) is the effect of coupling to the two-phonon excitation in the projectile (only the $[2_1^+ \otimes 2_1^+]$ two-phonon state was included). Both these calculations have been shifted up in energy by 1.0 MeV to account for the adiabaticity of the projectile coupling [21,35]. Coupling to the first excited state in the projectile does not dramatically alter the shape of the barrier distribution from the calculation which includes target excitations
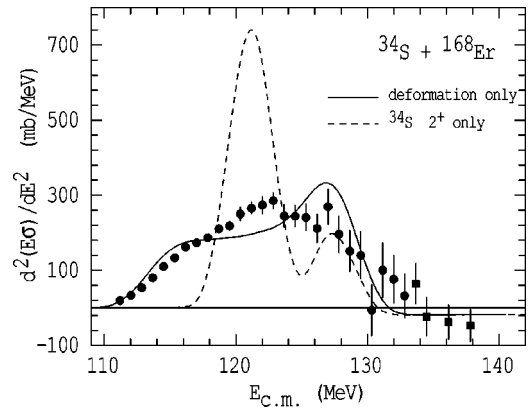
only. The single-phonon excitation in the target produces a second peak in the barrier distribution centered around 133 MeV, but the uncertainty on $d^2(E_{c.m.}\sigma)/dE_{c.m.}^2$ is too large to identify such a feature.

Coupling to the first excited state in ^{34}S has a small effect because the strong coupling from ^{168}Er produces a very broad barrier distribution. This means that the overall change in the shape of the barrier distribution is small, even though projectile coupling by itself produces a significant feature. This can be seen in Fig. 6, where a calculation with projectile coupling only is compared to a calculation which considers the target deformation only.

Two other calculations were performed, again with $\beta_2^T = 0.338$ and $\beta_6^T = +0.025$ for ^{168}Er. The first included coupling to the 3_1^- state in ^{34}S at an excitation energy of 4.62 MeV and $\beta_3^P = 0.388$ [33]. Coupling to this state only shifted the barrier distribution in energy, leaving its shape largely unchanged, as expected for a state which has such a large excitation energy [21,35]. In the other calculation, inclusion of the 2_1^+ state in ^{34}S and $\beta_2^T = 0.338$ and $\beta_6^T = -0.025$ for ^{168}Er, the theoretically predicted sign for the hexacontatetrapole deformation, produced a barrier distribution that in no way resembled the measured shape (calculation not shown). No reasonable combination of coupling to states in the projectile and the predicted value for β_6^T in ^{168}Er could be found to reproduce the desired shape of the measured barrier distribution.

(5) Coupling to transfer channels. Other weaker couplings not yet taken into account include transfer channels. The effective Q values, that is after taking into account the change in $Z_1 Z_2$ of the transfer products (where relevant), for various transfer channels are shown in Table III. Most of these transfer channels have a negative effective Q value, and the effect of their inclusion in a CC calculation would be to produce barriers with energies greater than the average fusion barrier [36]. However, in the presence of the strong collective couplings in ^{168}Er, the influence of the negative effective Q value transfers on the shape of the barrier distribution is likely to be small [6], as was seen with the inclusion of the inelastic excitations in ^{34}S in Sec. IV 4. With the CC code used in this analysis it was not possible to calculate

TABLE III. Summary of the effective Q values Q_{eff}, for various transfer channels for the reaction $^{34}\text{S}+{}^{168}\text{Er}$.

Transfer products	Channel	Q_{eff} (MeV)
$^{35}\text{S}+{}^{167}\text{Er}$	n pickup	-0.79
$^{33}\text{S}+{}^{169}\text{Er}$	n stripping	-5.4
$^{35}\text{Cl}+{}^{167}\text{Ho}$	p pickup	-7.4
$^{33}\text{P}+{}^{169}\text{Tm}$	p stripping	$+0.74$
$^{36}\text{Cl}+{}^{166}\text{Ho}$	d pickup	-6.2
$^{32}\text{P}+{}^{170}\text{Tm}$	d stripping	-2.8
$^{36}\text{S}+{}^{166}\text{Er}$	$2n$ pickup	$+2.7$
$^{32}\text{S}+{}^{170}\text{Er}$	$2n$ stripping	-6.8

correctly the effects of all the above transfer channels. However, a calculation was performed including the $2n$ pickup channel, since the macroscopic form factor assumed for this pair transfer is likely to be close to the results from a microscopic treatment [37]. Coupling to the pair transfer was made using the form factor

$$F_{\text{tran}}(R,\theta)=-\sigma_t(1+\beta_2^T Y_{20}+\beta_4^T Y_{40}+\beta_6^T Y_{60})\frac{dV(R,\theta)}{dR},$$

(4)

where R is the radius of the deformed target nucleus, θ is the orientation angle of the deformed (axially symmetric) target nucleus, and $Y_{\lambda 0}$ are the spherical harmonics. In Eq. (4), σ_t is the transfer strength parameter.

The results are shown by the dashed line in Fig. 7 which, in addition to the β_2^T and β_6^T deformation, with $\beta_2^T=0.338$ and $\beta_6^T=+0.025$, includes coupling to the $2n$ transfer channel with $Q=+2.7$ MeV and $\sigma_t=0.2$ MeV, the latter based on previous estimates of the pair transfer coupling strength [7,37]. The effect of the positive Q $2n$ pickup channel is to redistribute some barrier strength in the barrier distribution, although the overall shape of the barrier distribution is not changed significantly. For comparison, the dot-dashed line in Fig. 7 shows the effect on the barrier distribution when the
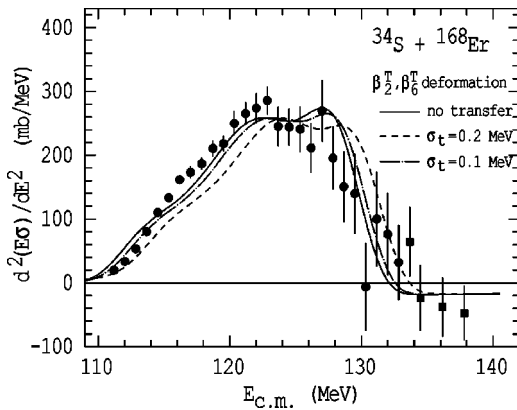

FIG. 7. Barrier distributions with $\beta_2^T=0.338$ and $\beta_6^T=+0.025$ and the $2n$ pickup transfer channel with $\sigma_t=0.2$ MeV (dashed line), $\sigma_t=0.1$ MeV (dot-dashed line), and without the transfer channel (solid line). Note that none of the barrier distributions in this figure have been shifted in energy.

transfer coupling strength is reduced to $\sigma_t=0.1$ MeV. An increase in the transfer strength parameter resulted in an increase in the width of the barrier distribution, producing a distribution wider than the experimental one. A calculation with $2n$ pickup channel and the theoretically predicted sign for β_6^T resulted in barrier distribution that was even more peaked than that shown by the dot-dashed line in Fig. 4(c). Neither of these calculations are shown.

As found in Sec. IV 4, no reasonable combination of weak coupling, in this case the $2n$ transfer channel, and the theoretically predicted sign for β_6^T (i.e., negative sign) could mimic the shape of the barrier distribution obtained for a positive value of β_6^T. It seems unlikely that coupling to known additional transfer channels could change the shape of the $^{34}\text{S}+{}^{168}\text{Er}$ barrier distribution to the extent the β_6^T in ^{168}Er does and thus account for the barrier distribution shape without resorting to the inclusion of β_6^T in the CC calculations.

V. SUMMARY AND CONCLUSION

Detailed coupled-channels calculations have been performed in an attempt to describe the shape of the recently measured barrier distribution [17,18] for the $^{34}\text{S}+{}^{168}\text{Er}$ reaction. The ^{168}Er nucleus was chosen to investigate the disagreement between theory and measurement at energies 1 or 2 MeV below the average barrier observed in a range of reactions on deformed target nuclei. Since ^{168}Er has a very small hexadecapole deformation, and because the 3_1^- state in ^{168}Er couples very weakly, it was expected that the presence of the quadrupole deformation alone would allow for a stringent test of the fusion model.

The calculated shape of the barrier distribution from a coupled channels calculation which included the quadrupole deformation only, failed to match the experimental $^{34}\text{S}+{}^{168}\text{Er}$ barrier distribution. Agreement with the experiment was improved significantly when the hexacontatetrapole deformation was included, with $\beta_6^T=+0.025$. However, this value for β_6^T has a sign opposite to that predicted in the macroscopic-microscopic model of Möller et al. [32].

When the theoretically predicted value for β_6^T was used, this resulted in a double-peaked barrier distribution in contrast with the data. No combination of coupling to low-lying states in the projectile and/or the $2n$ transfer channel, when using the theoretically predicted value for β_6^T, could reproduce the shape of the experimental barrier distribution. The best reproduction was obtained with a positive value for β_6^T. It was argued that if such higher-order deformations were to be visible in the fusion barrier distribution, then the ^{168}Er nucleus is likely to be one of the best candidates to observe their presence, since it has a very small hexadecapole deformation.

Within the framework of current fusion models, the fusion barrier distribution for $^{34}\text{S}+{}^{168}\text{Er}$ apparently defines the β_6^T deformation of ^{168}Er as positive, in contrast with theoretical predictions. Further theoretical investigations are warranted, which could also examine the possible influence on fusion of other higher-order deformations not considered in this analysis.

[1] C. Y. Wong, Phys. Lett. **42B**, 186 (1972).

[2] L. C. Vaz and J. M. Alexander, Phys. Rev. C **10**, 464 (1974).

[3] C. H. Dasso, S. Landowne, and A. Winther, Nucl. Phys. **A405**, 381 (1983).

[4] N. Rowley, G. R. Satchler, and P. H. Stelson, Phys. Lett. B **254**, 25 (1991).

[5] C. R. Morton, M. Dasgupta, D. J. Hinde, J. R. Leigh, R. C. Lemmon, J. P. Lestone, J. C. Mein, J. O. Newton, H. Timmers, N. Rowley, and A. T. Kruppa, Phys. Rev. Lett. **72**, 4074 (1994).

[6] J. R. Leigh, M. Dasgupta, D. J. Hinde, J. C. Mein, C. R. Morton, R. C. Lemmon, J. P. Lestone, J. O. Newton, H. Timmers, J. X. Wei, and N. Rowley, Phys. Rev. C **52**, 3151 (1995).

[7] R. A. Broglia, C. H. Dasso, and S. Landowne, Phys. Rev. C **32**, 1426 (1985).

[8] M. Dasgupta, D. J. Hinde, N. Rowley, and A. M. Stefanini, Annu. Rev. Nucl. Part. Sci. **48**, 401 (1998).

[9] J. X. Wei, J. R. Leigh, D. J. Hinde, J. O. Newton, R. C. Lemmon, S. Elfström, J. X. Chen, and N. Rowley, Phys. Rev. Lett. **67**, 3368 (1991).

[10] R. C. Lemmon, J. R. Leigh, J. X. Wei, C. R. Morton, D. J. Hinde, J. O. Newton, J. C. Mein, M. Dasgupta, and N. Rowley, Phys. Lett. B **316**, 32 (1993).

[11] P. R. Christensen and A. Winther, Phys. Lett. **65B**, 19 (1976).

[12] D. J. Hinde, M. Dasgupta, J. R. Leigh, J. P. Lestone, J. C. Mein, C. R. Morton, J. O. Newton, and H. Timmers, Phys. Rev. Lett. **74**, 1295 (1995).

[13] J. C. Mein, D. J. Hinde, M. Dasgupta, J. R. Leigh, J. O. Newton, and H. Timmers, Phys. Rev. C **55**, R995 (1997).

[14] T. Rumin, K. Hagino, and N. Takigawa, Phys. Rev. C **61**, 014605 (1999).

[15] D. L. Hendrie, N. K. Glendenning, B. G. Harvey, O. N. Jarvis, H. H. Duhm, J. Saudinos, and J. Mahoney, Phys. Lett. **26B**, 127 (1968).

[16] S. G. Nilsson, C. F. Tsang, A. Sobiczewski, Z. Szymański, S. Wycech, C. Gustafson, I. Lamm, P. Möller, and B. Nilsson, Nucl. Phys. **A131**, 1 (1969).

[17] C. R. Morton, A. C. Berriman, R. D. Butt, M. Dasgupta, A. Godley, D. J. Hinde, and J. O. Newton, Phys. Lett. B **481**, 160 (2000).

[18] C. R. Morton, A. C. Berriman, R. D. Butt, M. Dasgupta, A. Godley, D. J. Hinde, and J. O. Newton, Phys. Rev. C **62**, 024607 (2000).

[19] K. Hagino, N. Takigawa, M. Dasgupta, D. J. Hinde, and J. R. Leigh, Phys. Rev. C **55**, 276 (1997).

[20] A. M. Stefanini, L. Corradi, A. M. Vinodkumar, Yang Feng, F. Scarlassara, G. Montagnoli, S. Beghini, and M. Bisogno, Phys. Rev. C **62**, 014601 (2000).

[21] C. R. Morton, A. C. Berriman, M. Dasgupta, D. J. Hinde, J. O. Newton, K. Hagino, and I. J. Thompson, Phys. Rev. C **60**, 044608 (1999).

[22] J. O. Newton, C. R. Morton, M. Dasgupta, J. R. Leigh, J. C. Mein, D. J. Hinde, H. Timmers, and K. Hagino, Phys. Rev. C (submitted).

[23] ANU unpublished data.

[24] S. Raman, C. H. Malarkey, W. T. Milner, C. W. Nestor, Jr., and P. H. Stelson, At. Data Nucl. Data Tables **36**, 1 (1987).

[25] K. Hagino (unpublished).

[26] K. Hagino, N. Rowley, and A. T. Kruppa, Comput. Phys. Commun. **123**, 143 (1999).

[27] R. Lindsay and N. Rowley, J. Phys. G **10**, 805 (1984).

[28] O. Tanimura, J. Makowka, and U. Mosel, Phys. Lett. **163B**, 317 (1985).

[29] O. Tanimura, Phys. Rev. C **35**, 1600 (1987); Z. Phys. A **327**, 413 (1987).

[30] M. A. Nagarajan, A. B. Balantekin, and N. Takigawa, Phys. Rev. C **34**, 894 (1986).

[31] T. Rumin, K. Hagino, and N. Takigawa, Phys. Rev. C **63**, 044603 (2001).

[32] P. Möller, J. R. Nix, W. D. Myers, and W. J. Swiatecki, At. Data Nucl. Data Tables **59**, 185 (1995).

[33] R. H. Spear, At. Data Nucl. Data Tables **42**, 55 (1989).

[34] H. G. Börner, J. Jolie, S. J. Robinson, B. Krusche, R. Piepenbring, R. F. Casten, A. Aprahamian, and J. P. Draayer, Phys. Rev. Lett. **66**, 691 (1991).

[35] K. Hagino, N. Takigawa, M. Dasgupta, D. J. Hinde, and J. R. Leigh, Phys. Rev. Lett. **79**, 2014 (1997).

[36] C. H. Dasso, S. Landowne, and A. Winther, Nucl. Phys. **A407**, 221 (1983).

[37] C. H. Dasso and G. Pollarolo, Phys. Lett. **155B**, 223 (1985).